Available online at www.CivileJournal.org

Civil Engineering Journal

(E-ISSN: 2476-3055; ISSN: 2676-6957)

Vol. 9, No. 08, August, 2023

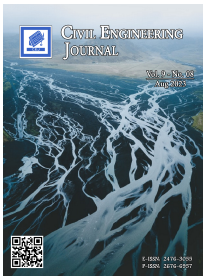

Post Fire Behavior of Structural Reinforced Concrete Member (Slab) Repairing with Various Materials

Asser Elsheikh [1, 2*], Hadeal H. Alzamili [1]

[1] *Department of Civil Engineering, Peoples' Friendship University of Russia (RUDN), Moscow, Russian Federation.*

[2] *Structural Engineering Department, Mansoura University, Mansoura, Egypt.*

Received 27 April 2023; Revised 09 July 2023; Accepted 18 July 2023; Published 01 August 2023

Abstract

One of the most significant building materials used to build a variety of infrastructure, military, and civil structures is concrete. It can effectively withstand fire mishaps for a long period of time. This study employs a finite element simulation approach in Three steps: the first involves applying mechanical loading, the second involves applying mechanical and thermal loading; and the third involves strengthening the damaged model. Two different strengthening procedures were used to evaluate the performance of the fire-damaged slab. Two types of strengthening techniques—carbon-fiber-reinforced polymer (CFRP) sheet and slurry-infiltrated fibrous concrete (SIFCON) jacketing—were used. Studying the performance of SIFCON and CFRP together and in two different thicknesses of each for repairing both normal and high-strength concretes after fire exposure is considered limited. An investigation of their behavior can provide insights into how effective the restoration of strength is. The study aims to assess how well various repair materials perform in restoring the durability and strength of reinforced concrete members after being exposed to fire. This will assist in determining the best materials for concrete repair after a fire. Results show that the enhancements by SIFCON with a thickness of 30 mm significantly improved many indices, including load displacement behavior, ductility, and absorption energy of the slab.

Keywords: RC Slab; CFRP; SIFCON; Stiffness; Ductility; Absorption Energy; CDP.

1. Introduction

Buildings made of concrete are prone to fire damage. When exposed to extreme temperatures, concrete slabs can lose strength, the concrete cover can break off, crack, and lose steel reinforcing. Effective repairs must be performed on fire-damaged concrete slabs for them to regain their structural performance and service life. Concrete repairs are traditionally carried out using proprietary repair mortars and concrete overlays. These adjustments might not completely restore the original concrete's properties, and durability issues might persist. For strengthening and rebuilding concrete structures, more recent materials like fiber-reinforced polymer composites and fiber-reinforced concrete have shown promise. In repairing concrete slabs that have been damaged by fire effectively. Zhou & Wang (2019) concluded that when an existing structure begins to deteriorate or needs to be altered so that it can no longer fulfill its intended function, strengthening concrete structures must be taken into consideration, as must the loads while strengthening and the damaged condition of existing materials [1]. Balamurugan et al. (2020) investigated all failure modes must be assessed before undertaking structural strengthening of concrete. When a structure is strengthened for flexure, the result may be shear failure rather than the expected improvement in load-bearing capacity [2].

* Corresponding author: assermfee@mans.edu.eg

http://dx.doi.org/10.28991/CEJ-2023-09-08-013

Bezerra et al. (2019) investigated the impact of high temperatures on the mechanical characteristics of concrete reinforced with steel fibers of different aspect ratios. They used four different concrete mixtures and cured them for 28 days. The specimens were annealed in an electric furnace for three hours at a temperature of 500 °C after curing and natural drying. They concluded that the mechanical properties of steel fiber-reinforced concrete (particularly flexural toughness) were less influenced by high temperatures. After being subjected to high temperatures, the study's test results show that adding steel fibers to concrete-based composites greatly improves both fire and sound resistance [3].

Zhang et al. (2019) employed in this investigation large-scale tests on six separate slab-column connection specimens; each specimen has a 150 mm thick slab and a 300 mm square center column. High temperatures were applied to slab shear-critical areas at the compressive face using ceramic fiber heating panels. The test findings show that connection punching shear strength was unaffected by high temperatures up to 800 °C. Moreover, the use of crossties can reduce the failure rate of the chilled slab-column connections by up to 11% by effectively engaging the slab's tensile reinforcement in resisting post-punching loads with a loading capacity close to or even larger than the punching failure load [4].

1.1. Reinforced Concrete Slabs Strengthening with SIFCON/CFRP

Abdulah (2015) reported that the ultimate loads and capacity of the externally reinforced concrete two-way slabs with bonded CFRP sheets significantly increased when compared to the un-strengthened (control) slabs, increasing by around 7–45% depending on the type of strengthening [5]. Sui et al. (2020) investigated the flexural behavior of CFRP-versus-TRM-strengthened fire-damaged prefabricated RC hollow slabs. They strengthened fire-damaged prefabricated concrete hollow slabs using CFRP and textile reinforced mortar (TRM) techniques, and they revealed that both CFRP and TRM strengthening techniques can greatly raise the cracking load, peak load, and initial stiffness of fire-damaged hollow slabs [6]. Huang et al. (2020) present one control steel-reinforced concrete (RC) slab and five CFRP-reinforced concrete slabs that were included in the six full-scale 1600 × 1600 × 150 mm slab specimens that were constructed and tested under monotonic stress until failure. The findings indicate that adding more shear CFRP grids can make concrete slabs more resistant to being punched. When compared to typical non-shear reinforcement slabs, the load-bearing capacity rises by 17.9% to 27.4%, and the deformation rises by 11.1% to 49.0% [7]. In order to determine the best mixture proportions of highly workable slurry composites with high strength for SIFCON applications, an experimental study on ultra-high strength slurry infiltrating multiscale fiber-reinforced concrete was reported by Mohan et al. (2020) in this paper. Evaluations were made of the mechanical characteristics, such as compressive strength, of water-cured specimens tested at 3, 7, 28, and 28 days for rapid curing cube specimens. Flexural behavior experiments were run on $50 \times 500 \times 25$mm SIFCON slabs that had been cured quickly [8].

In order to assess several mechanical properties of SIFCON (Slurry Infiltrated Fibrous Concrete), including flexural, compressive, and splitting strength, Al-Abdalay et al. (2020) investigated the study by using plate specimens measuring 450mm by 100mm by 40mm and made of micro-steel fiber with a 6% volume percentage. These specimens were evaluated under impact load and compared to reference plates after 90 days. According to the findings of the experiment, SIFCON specimens performed significantly better than ordinary mortar, and when compared to traditional mortar, SIFCON exhibits improved strength in the "compressive, splitting, and flexural" tests for all ages (reference) [9].

Many studies have been done on the post-fire behavior of structurally reinforced concrete members (slabs) repaired with one technique, such as fiber-reinforced polymer (FRP), glass-reinforced polymer (GFRP), carbon-reinforced polymer (CFRP), normal-strength concrete (NSC), fiber-reinforced concrete (FRC), shotcrete, and Ferro cement. However, the application of various techniques in the same study is limited and has not received much attention.

Although prior research has provided insight into the post-fire behavior of reinforced concrete elements repaired using a variety of techniques, there are still knowledge gaps in the following areas:

- Evaluating the efficacy of various repair materials;
- Assessing a wide range of performance metrics;
- Testing members with different configurations;
- Developing standards for material selection;
- Understanding performance under various fire exposures.

Therefore, in this study (SIFCON and CFRP), two parameters (two thicknesses for SIFCON and CFRP) were also gathered for each strengthening type. The effectiveness of the orientation of CFRP and SIFON on two-way RC slabs with an adequate covering area should also be evaluated, as should the performance characteristics of toughness, ductility, and stiffness that go along with them.

2. Methods and Materials Models

2.1. Methods

Figure 1 clarifies the obtained results shall be presented in details as main two parts.

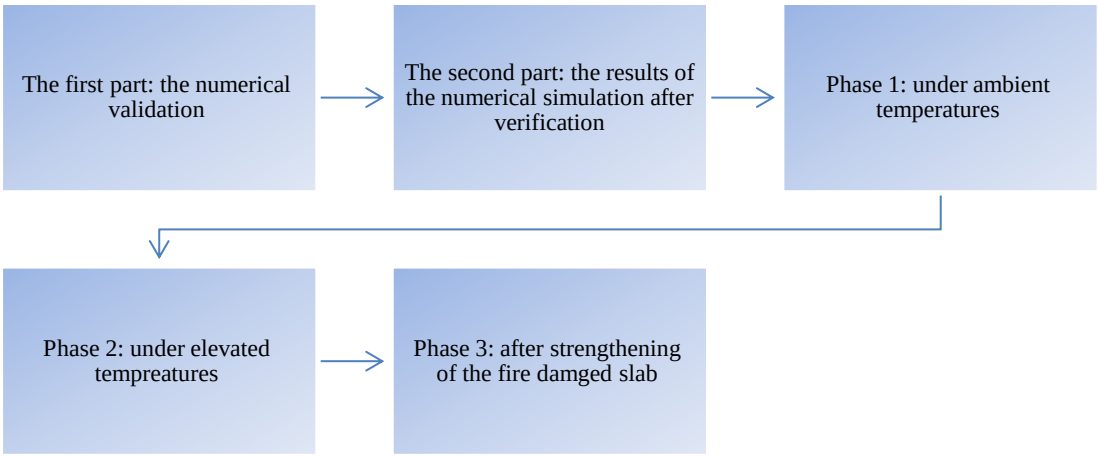

Figure 1. Methodology used

Here is a breakdown of the three phases mentioned in modeling and simulating the concrete slab samples:

Phase A: Modeling and simulating the reference samples (unfired concrete elements, without enhancement): In this phase, finite element models will be created for the concrete beam samples under study in their original, unfired state, the models will represent the geometrical and material properties of the as-cast concrete slabs, including the reinforcing steel bars, Static and dynamic load cases will be applied to the models to simulate the behavior and response of the unfired concrete slabs under different loading and boundary conditions.

Phase B: Simulating the concrete slab samples subjected to high temperatures without enhancement: In this phase, the same finite element models will be modified to represent the effects of exposure to high temperatures, simulating a fire, the models will incorporate changes in material properties, like strength reduction and stiffness degradation, to represent the behavior of the concrete and reinforcing steel after exposure to fire, the loaded models will then be simulated again to determine how the behavior and response of the slabs have changed after exposure to high temperatures.

Phase C: Modeling and simulating the fired concrete slab after enhancement: In the final phase, the finite element models will be further modified to represent the enhancement or repair techniques being investigated. The models will incorporate the material properties of the enhancement materials and their interaction with the original concrete. The loaded and constrained models will then be simulated again to determine the effectiveness of the enhancement techniques in restoring or improving the structural performance of the fired concrete slabs.

Generally speaking, to simulate any process or behavior of concrete elements, some main processes should pass through while suing ABAQUS, as follows:

1. Parts modeling: in this step, the geometrical modeling of the part's simulation can be created.
2. Material property: in this step, the properties of the used concrete and steel parts are characterized and assigned. Additionally, the properties of the materials used as enhancement agents shall be presented and detailed for SIFCON and CFRP materials.
3. Assembly: to assemble and collect all parts involved in the simulation process.
4. Step: to define the type of analysis, duration of the simulation process, and solver configuration.
5. Constraints and interactions properties: to specify the type and nature of the interacted surface, in addition to specifying the properties of the interface.
6. Loading and boundary conditions: to assign the type of loading (mechanical, thermal, electrical, etc.) and boundary condition states of the samples
7. Predefined field: to define the initial status of the assembly in terms of stress, temperature distribution, etc.
8. Job: to perform and start the simulation process.

In this paper, finite element modeling with ABAQUS was used; the modeling and simulation phases for the samples will be covered in detail.

Complex Geometry: Concrete structures have complex geometries with reinforcing bars, Nonlinear material behavior - Concrete exhibits nonlinear stress-strain behavior. Internal responses - Finite element models provide detailed information about the internal responses of concrete structures, such as stresses, strains and displacements. This data can provide insights into failure initiation and propagation, Multiple load cases - Different static and thermal load cases can be applied to the finite element model to simulate different usage scenarios and failure modes. This provides a comprehensive understanding of concrete behavior. Validation by compression against experimental data to validate the modeling assumptions and material models used. This ensures accurate predictions from the simulations. Predictions - Once validated, finite element models can be used to predict the behavior and performance of full-scale concrete structures that may be difficult or expensive to experimentally test.

2.2. Materials Models

ABAQUS offers a variety of material attributes that reflect how those materials behave under various simulation scenarios. Moreover, several theories of failure are offered for metals, soils, concrete, etc. Elastic and plastic phases are typically utilized to describe two phases for simulating concrete elements. The Poisson's ratio and the modulus of elasticity are two quantities that are frequently used to describe the elastic phase in isotropic materials [10].

The Concrete Damaged Plasticity Model (CDP) and the Concrete Smeared Cracks Model are the two models used to describe the concrete plastic phase. In order to define the plastic phase of quasi-brittle materials like concrete, Panahi et al. (2022) [11], Raza et al. (2019) [12], and Micha et al. (2015) [13] advocated using the CDP model due to its effectiveness in predicting concrete response under various scenarios, such as The characteristics of plain and reinforced concrete, monolithic and repetitive loadings, and application all depend on the rate at which the materials are loaded. The capacity of this model to predict isotropic elasticity as well as isotropic tensile and compressive damaged plasticity to represent the inelastic section is its most crucial component [14].

2.2.1. The concrete Damaged Plasticity Model Parameters in ABAQUS

Angle of dilation, eccentricity, surface plasticity flow number, viscosity, and the ratio of biaxial compressive strength to uniaxial compressive strength are the five essential parameters that must be established for the CDP model [15]. To define the failure surface envelope in three dimensions, the following parameters are required: Moreover, the tensile behavior (inelastic stress with cracking strain curve, beyond the cracking strength) as well as the compressive behavior (the inelastic compressive strength with plastic strain curve) must be entered [16]. The parameters of the CDP failure surface are shown in Table 1.

Table 1. The selected CDP material parameter for unfired concrete

Parameter	Selected value
Material model	CDP model
E, MPa	23500 MPa for C25 and 38000 MPa for C65
Possion’s ratio	Varied according to the temperature
Dilation angel	30 for C25 MPa and 40 for C65
*Ecc	0.1
*F_{b0}/f_{c0}	1.16
*K	2/3
*Viscosity parameter	0.001

* As recommended by Abaqus manual

The uniaxial unconfined stress-strain behavior under compressive and tensile loads at ambient temperature are two more significant curves that must be entered into the CDP model (20^{o}C). The unconfined compressive stress-strain of concrete in the normal and high strength classes is illustrated in Figure 2. These curves can be divided into two categories: elastic (defined by the modulus of elasticity and possion's ratio) and plastic (described by the CDP model). For both the tensile and compressive behaviors of concrete, the plastic phase is defined.

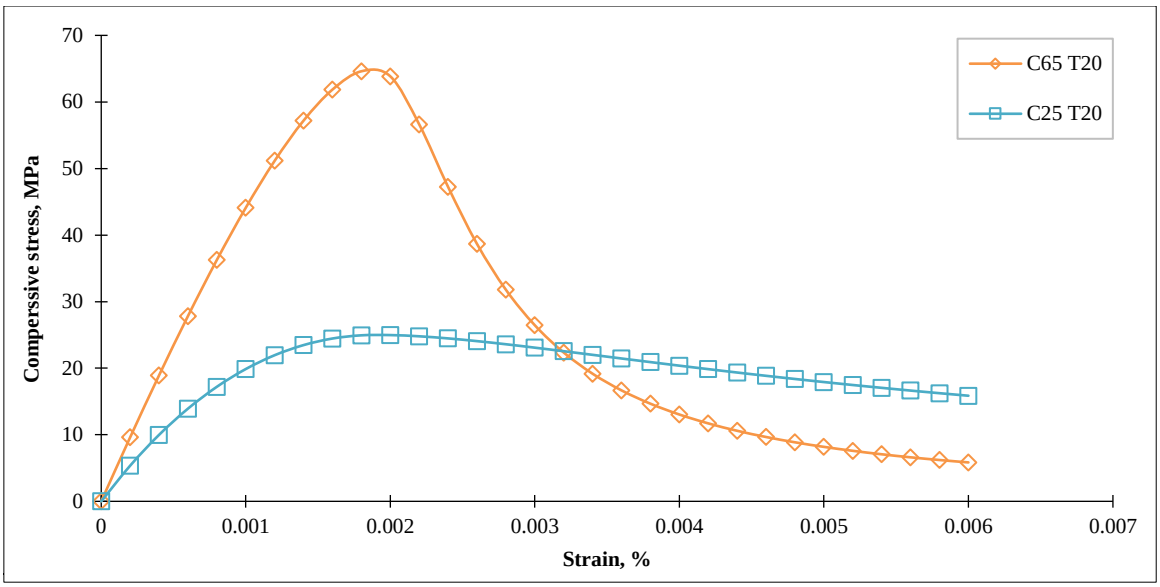

Figure 2. uniaxial concrete compressive stress- strain at ambient temperature (20°C) for normal (25 MPa) and high (65MPa) strength concrete class

2.2.2. Defining Steel Material Behavior

The engineering stress-strain relation, the true or logarithmic stress-strain relation, the elastic perfect plastic behavior, and the bilinear elasto-plastic with hardening are the four stress-strain models that are typically employed to characterize the behavior of steel materials [17]. The elastic modulus and reinforcement steel were simulated using the built-in bilinear kinematic reinforcement model of Abaqus. In this study, the perfect elastic plastic behavior for steel reinforcing rebars has been used. Due to this tendency, the elastic and plastic models must be defined with at least one point at yielding, which corresponds to zero plastic strain. On the other hand, the yield point and the rapture point are the minimum requirements for the linear hardening of the plastic phase [18].

3. Numerical Validation

First, and most importantly, confirmation with prior experimental work is essential before beginning any parametric investigation utilizing the finite element simulation. As a result, a prior study by Bin Cai et al. (2020) has been used as the basis for the validation procedure, with the geometrical configuration and material characteristics shown in Figures 3 and 4. Briefly stated, the goal of the aforementioned investigation was to determine how firing affected the concrete slab's performance after being exposed to heat for one hour. The materials were defined, put together, and loaded into ABAQUS after being geometrically modeled for all the data.

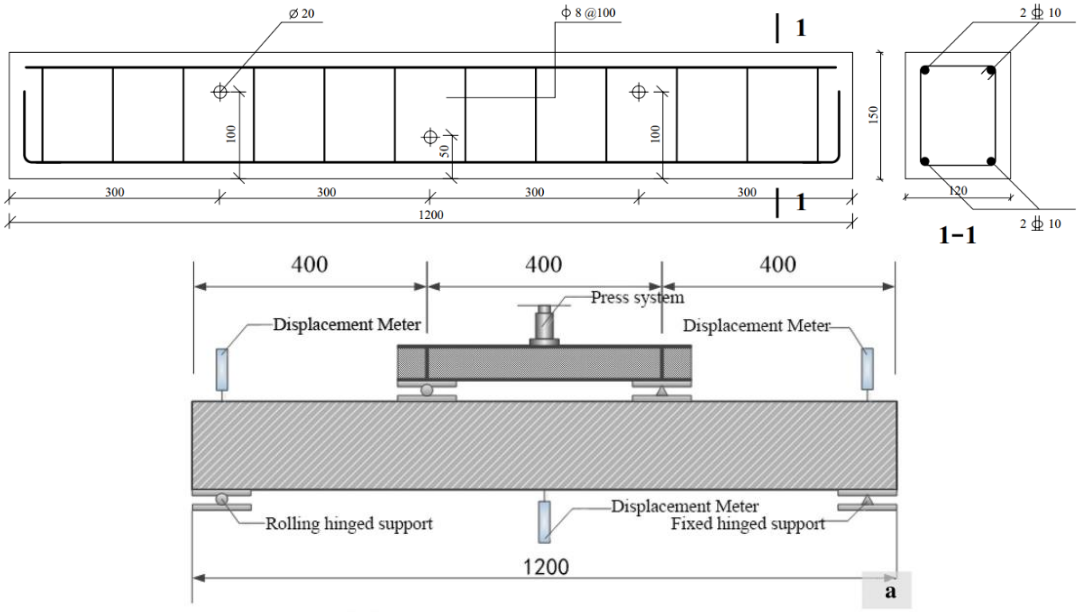

Figure 3. Geometric layout of the validated beam [19]

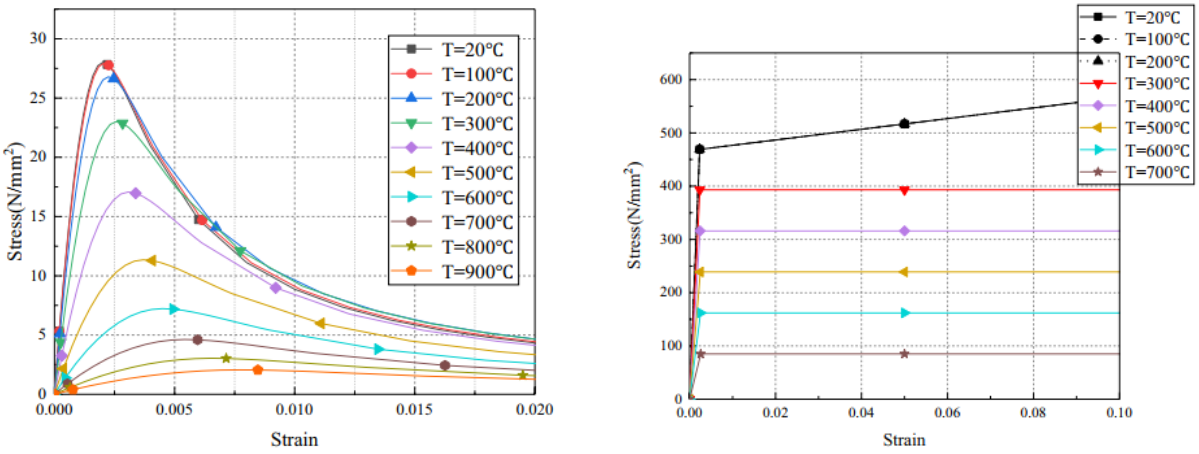

Figure 4. Properties of concrete and steel reinforcement of the validated research [19]

The outcomes of the validation tests demonstrated that the numerical validation curves were identical to the experimental test curves in regards to the load-mid-span displacement of the reference and fire-damaged concrete beam specimens, as shown in Figures 5 and 6. The maximum error between the maximum load-bearing capacity and the corresponding displacement values was less than 5%, which is considered to be extremely acceptable for validation results. Additionally, the behaviors of the curves in the elastic and plastic phases were essentially the same, particularly for the elastic phase of the validated, undamaged beam and the plastic phase of the damaged beam. According to the results, the chosen concrete qualities under different temperature ranges.

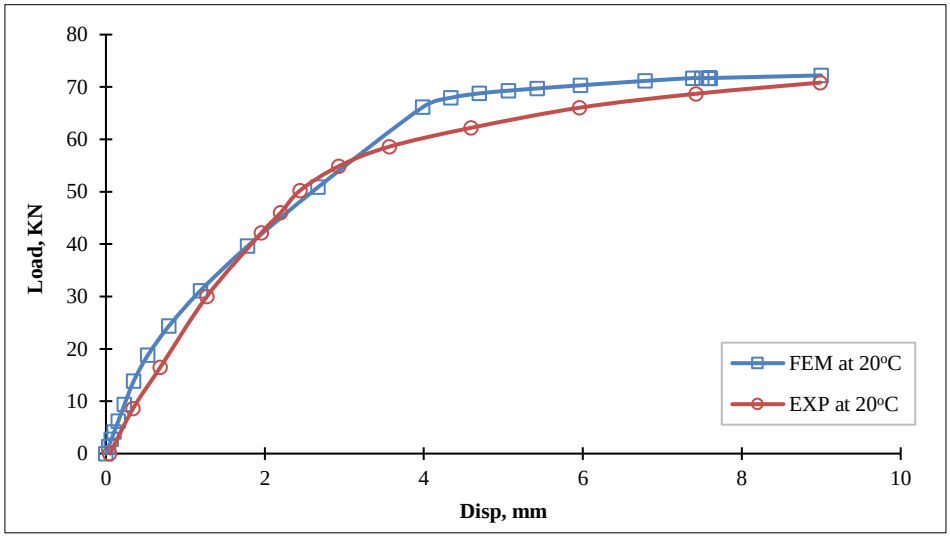

Figure 5. Experimental vs. numerical load-displacement curves at ambient temperatures

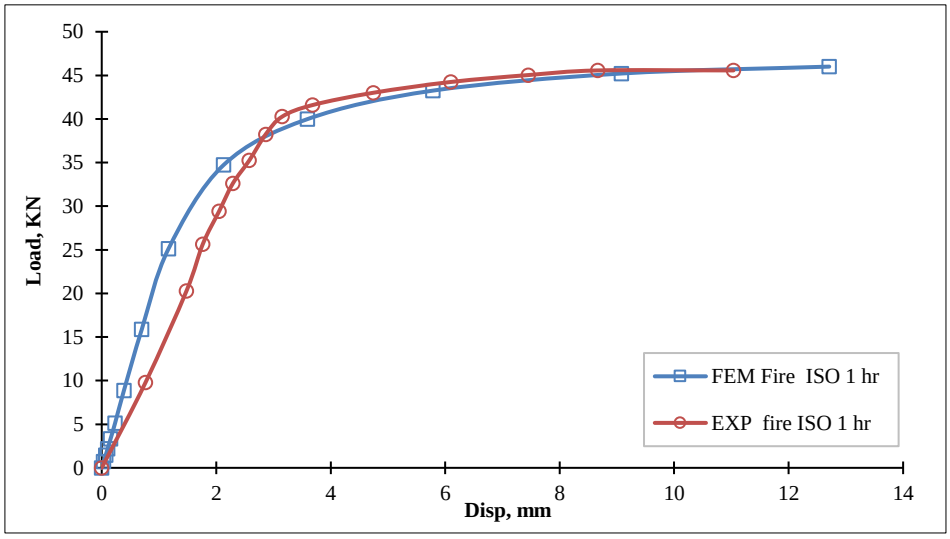

Figure 6. Experimental vs. numerical load-displacement curves after 1-hour firing

It is necessary to describe and discuss in detail the behavior of the slab under various heat conditions and repair methods in order to demonstrate the degree of degradation and improvement in the elements' performance as measured by various flexural indices. According to the kind of concrete strength (normal strength (N), high strength concrete (H), reference (R), fired (F), slab (S), and type of strengthening (SIFCON (SX), and CFRP (CFx), where X is the thickness of the layer), the slab as shown in Table 2 was designated.

Table 2. Adopted Concrete members' designation

Slab dimension	Type of concrete	Slab designation	Type of strengthens	Configuration of strengthen
Slab 5500 mm square with 200 mm depth	Normal concrete	S-R-N	-	-
	25 MPa (NSC)	S-F-N	-	-
		S-S20-N	SIFCON	20 mm
		S-S30-N	SIFCON	30 mm
		S-CF1.5-N	CFRP	one layer
		S-CF2.5-N	CFRP	two layer
	High concrete	S-R-H	-	-
	65 MPa (HSC)	S-F-H	-	-
		S-S20-H	SIFCON	20 mm
		S-S30-H	SIFCON	30 mm
		S-CF1.5-H	CFRP	one layer
		S-CF2.5-H	CFRP	two layer

To demonstrate the effect of fire impact that occurs frequently in some infrastructure facilities, such as hospitals, full-scale dimensions of the main concrete element (slab) were selected to ensure that its behavior is classified as a two-way action slab. The slab depth was 200 mm, and the aspect ratio was 1 (square slab), with dimensions of 5500 mm by 5500 mm. The embedded steel reinforcement was two meshes (top and bottom) using steel bars with a diameter of 12 mm and 200 mm, respectively. Figure 7 illustrates slab dimensions and steel reinforcement distribution.

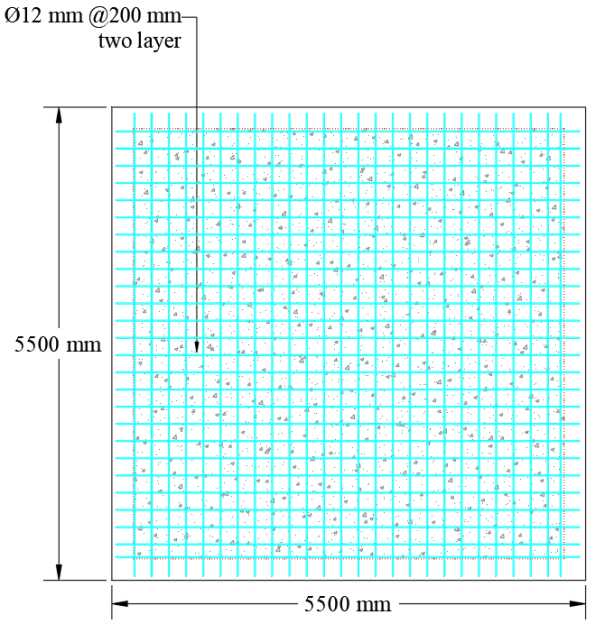

Figure 7. Slab dimensions and steel reinforcement distribution

4. FEM Analysis and Results

4.1. Thermal Distribution Map on the Concrete Slab and Steel Reinforcement

The thermal distribution due to exposing the slab bottom face to the ISO-834 standard fire curve criteria is simulated, presented, and detailed. For the concrete slab, after subjecting the bottom face to the ISO fire criteria for two hours during the thermal and heat transfer analysis, isothermal curves in some specific important locations have been generated, as can be seen in Figure 8. These points are located along the midline of the cross section and at various depths: at the bottom surface, at the steel reinforcement location, and at the midline of the concrete depth. It can be noticed that after one hour of firing, the temperature degrees were 69ºC, 338ºC, and 453ºC, respectively, for the mentioned point locations. After 2 hours, the temperature degrees were 157ºC, 502ºC, and 633ºC for the previously

mentioned points in the same manner. Moreover, the thermal distribution of the slab cross section after half an hour, one hour, one and a half hours, and two hours (A, B, and C) is illustrated in Figure 9. It should be noted that the slab corners suffered from the highest thermal concentration, which reached 895°C. In addition, the 3D view of the temperature distribution on the steel reinforcement showed that the bottom longitudinal bars reached 504°C after two hours. All of the mentioned temperature variations reflected the initial residual stress before the mechanical load and strengthening phase.

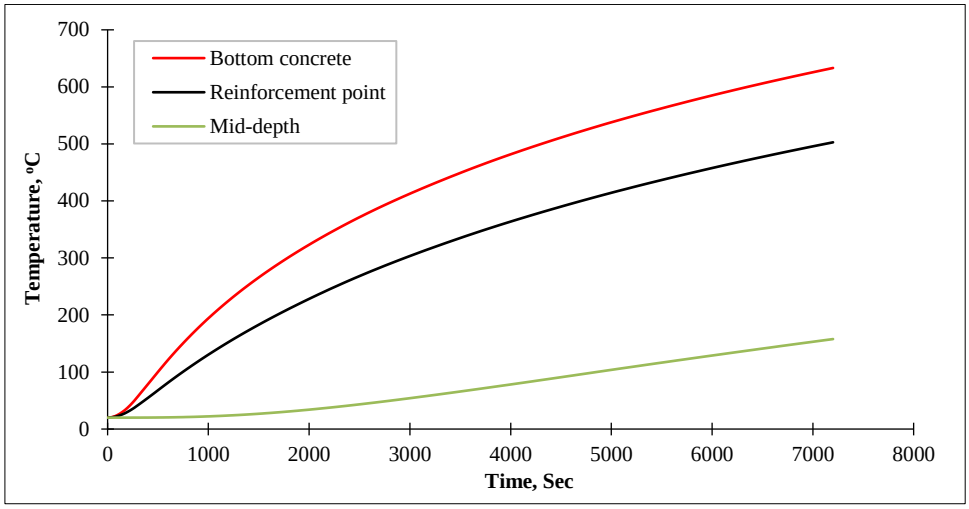

Figure 7. Isothermal curves at specified location in the slab cross section

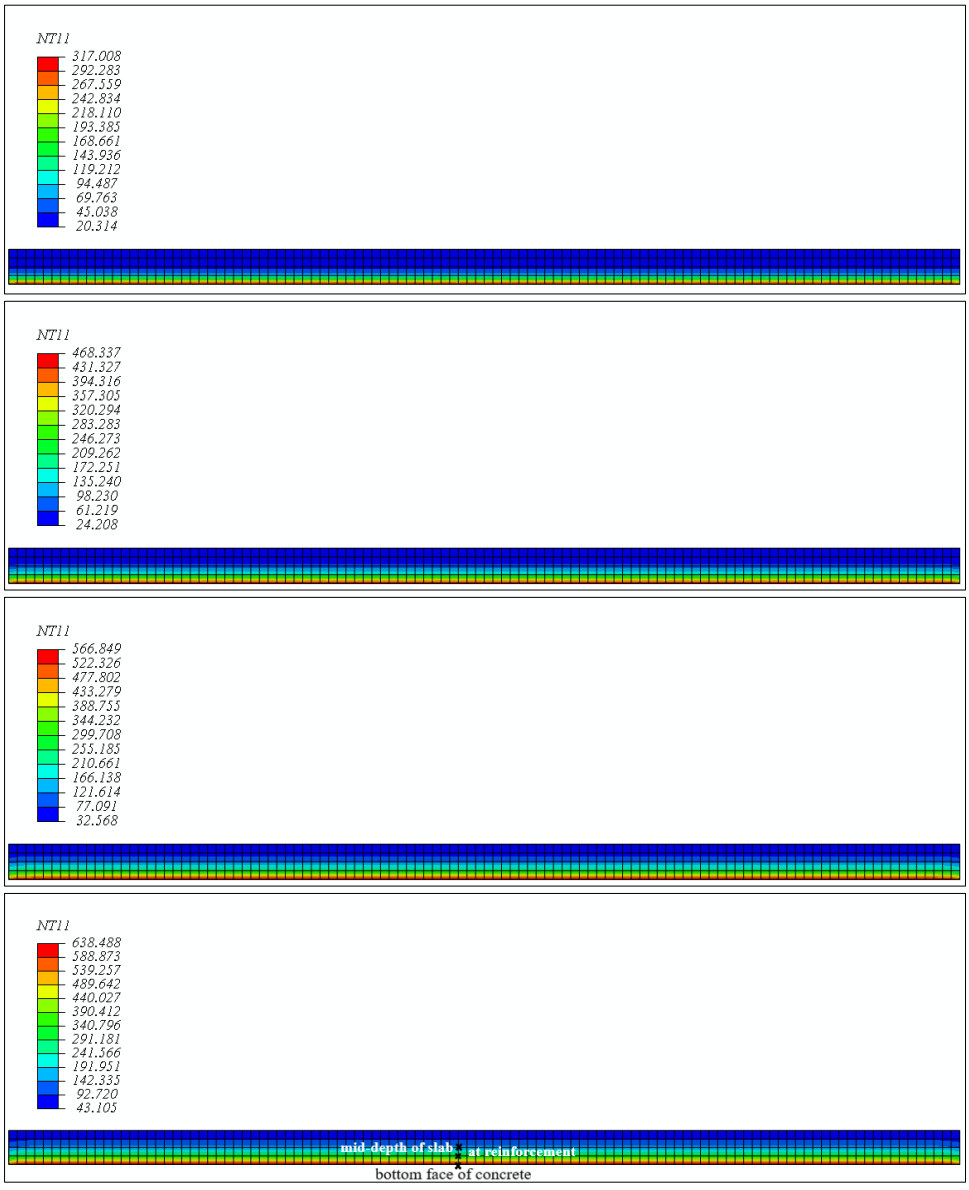

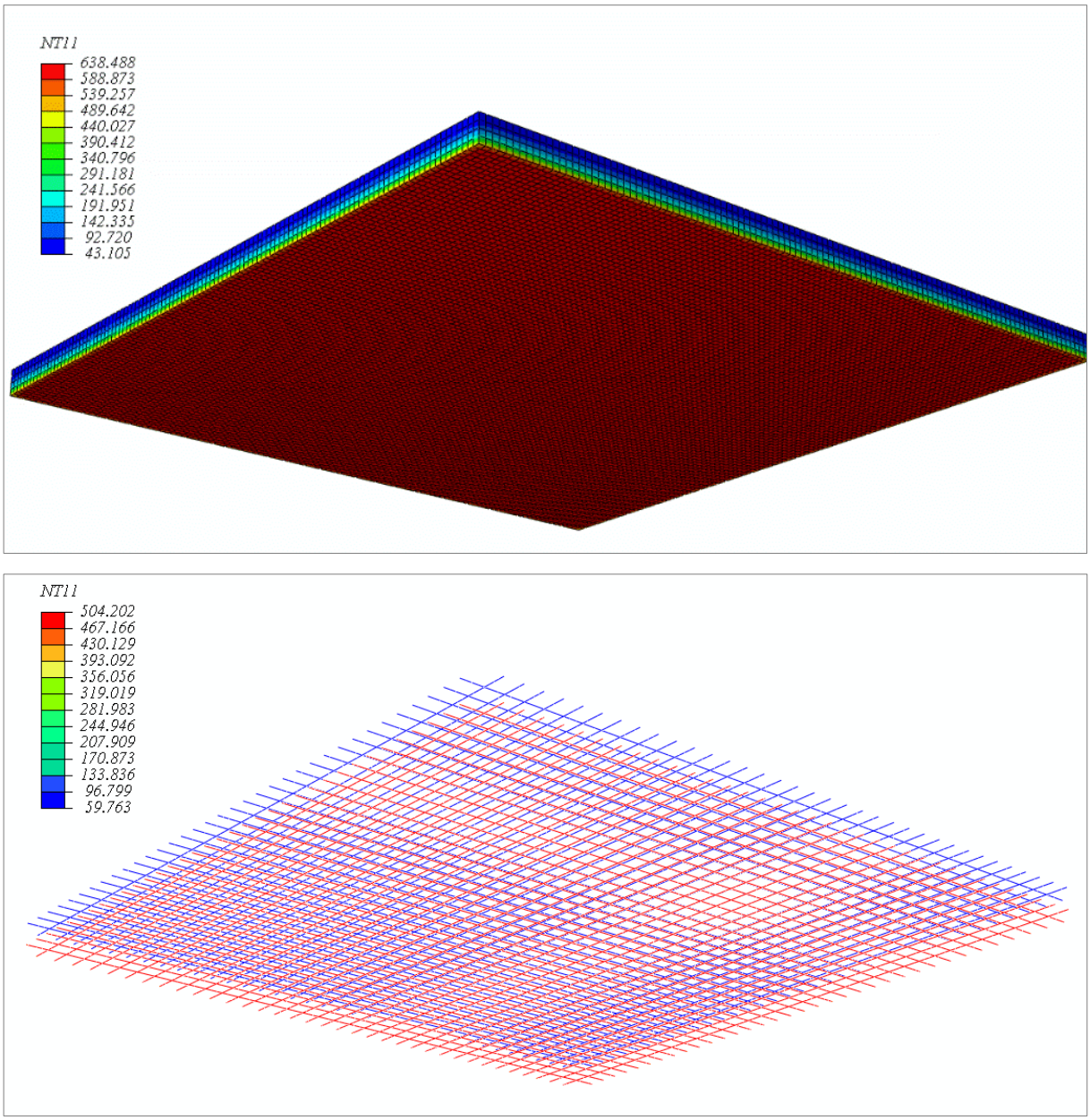

Figure 8. Temperature distribution on the slab cross section (from top to bottom) after A. half of an hour, one hour, one and half of hour, 2 hours. In addition to a 3D view of temperature distribution on the slab and steel reinforcement

4.1.1. Behavior of the Concrete Slab under Ambient and Elevated Temperatures

After subjecting the reference slab (the bottom face) to elevated temperatures, new behavior has appeared with a significant reduction in the load capacity, as can be seen in Figure 10, for the load-displacement behavior of the fire-damaged slab in addition to the reference model (normal strength). It can be clearly observed that a noticeable effect has been enhanced sufficiently. Compared with the reference slab, the ductility was reduced. The effect of fire may result in higher ductility, but all other indices are in contrast, as shall be discussed in the next subsection. The same behavior has been noticed for the high-strength slab concrete, but of course with different reduction percentages; see Figure 11, for the load displacement curves of the reference and fire-damaged high-strength slabs. It has been noticed that the reduction due to fire for normal-strength concrete in slabs is higher than what has been observed for high-strength concrete slabs. Moreover, the behavior of high-strength slabs for the reference and fire-damaged slabs was approximately the same.

For the ultimate load capacity, as illustrated in Figure 12, it has noticed a reduction in the load capacity index due to firing of about 30% and 17.5% for the normal and high-strength concrete slabs, respectively. Which means that the high-strength concrete slabs lost approximately half of their load capacity compared to the normal concrete slab.

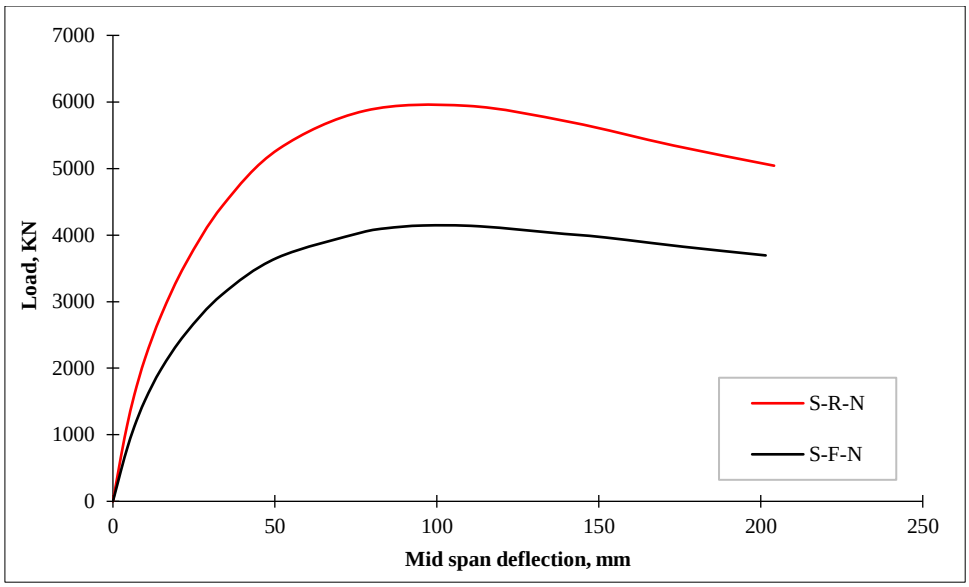

Figure 9. Load-displacement curves at ambient and elevated temperatures for the normal strength concrete slab

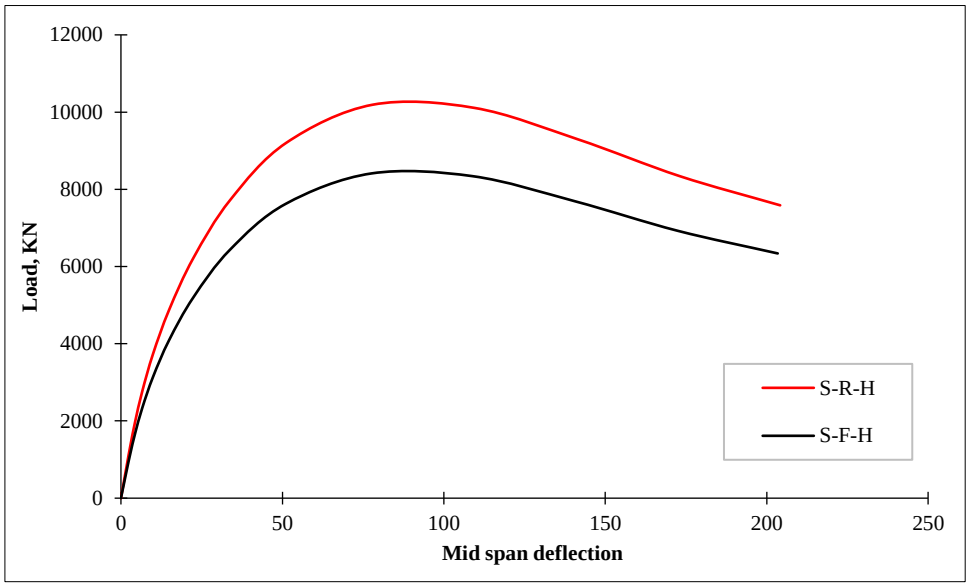

Figure 10. Load-displacement curves at ambient and elevated temperatures for the high strength concrete slab

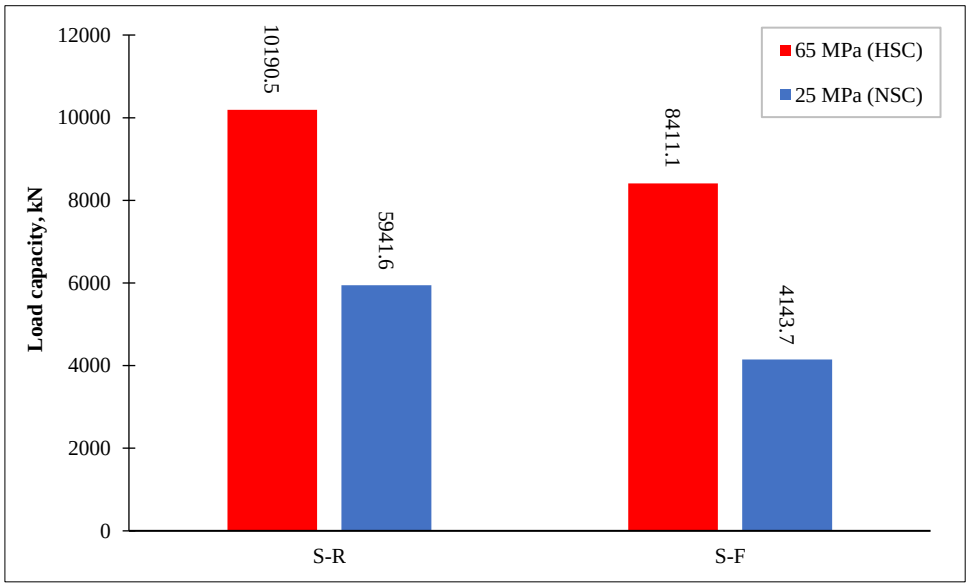

Figure 11. Ultimate load capacity of the reference and fire damaged concrete slab

Figure 13, illustrates the stiffness reduction of the normal and high-strength slab models due to fire damage. It can be noticed that, the same as for load capacity index, the normal strength slab reduction in stiffness was higher than the high strength concrete slab. Overall, a reduction in the stiffness values was about 46.7% and 20% for the normal and high strength types, respectively. which means that (in terms of stiffness index), the high-strength slab can resist fire by about 200% compared to the normal-strength slab.

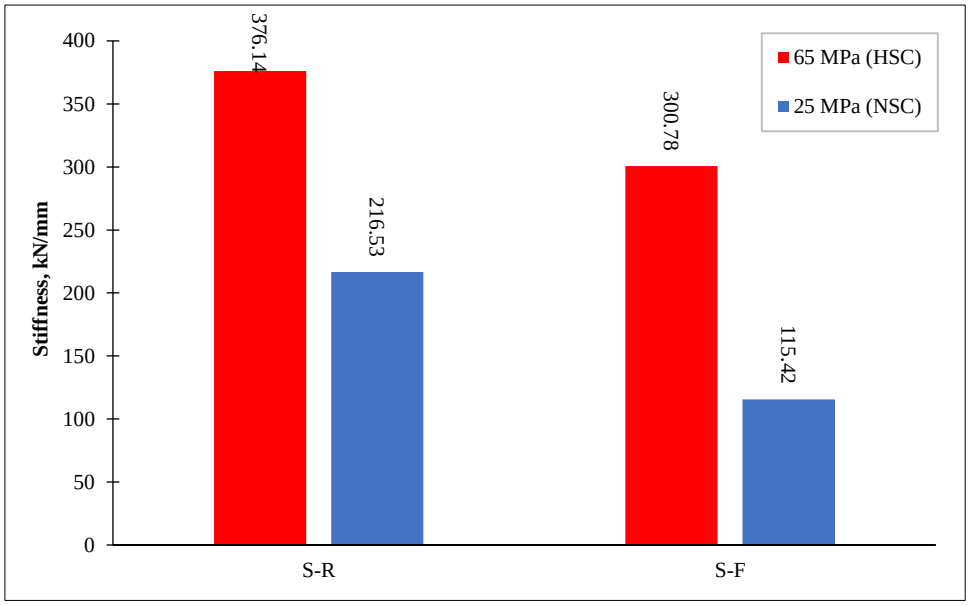

Figure 12. Effect of high temperatures on stiffness of the normal and high strength class concrete slab

The fire effect on the ductility index of the slab is illustrated in Figure 14. From the first view, it can be observed that the ductility of the normal strength slab is higher than that of the high-strength slab in both cases (before and after firing). The results show that a reduction in the normal and high-strength slabs was about 18.2% and 9%, respectively. which means approximately the same reduction in stiffness and load capacity.

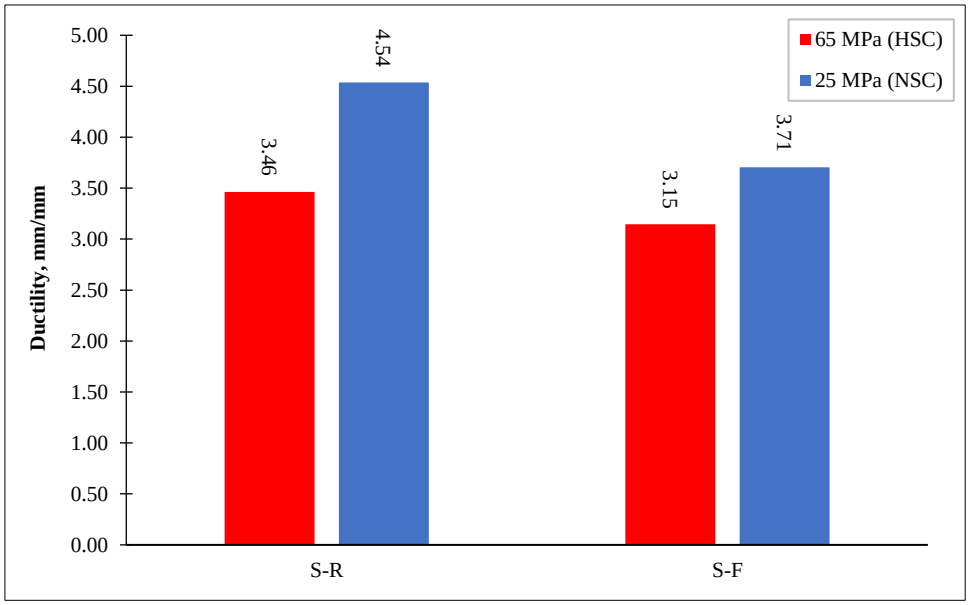

Figure 13. Effect of high temperatures on the ductility of the normal and high strength class concrete slab

In the case of absorption energy (KN.mm), as clarified in Figure 15, the difference in toughness between the reference normal and high strength concrete slab is about 15%, while the difference is about 36% for the normal strength slab in the same manner. Overall, the loss in toughness due to the fire effect duration of 2 hours was about 38.6% and 16.8% for normal and high-strength concrete, respectively. which means that the normal strength concrete has lost more than 200% of its absorption energy due to the fire effect when compared with the high-strength concrete slab.

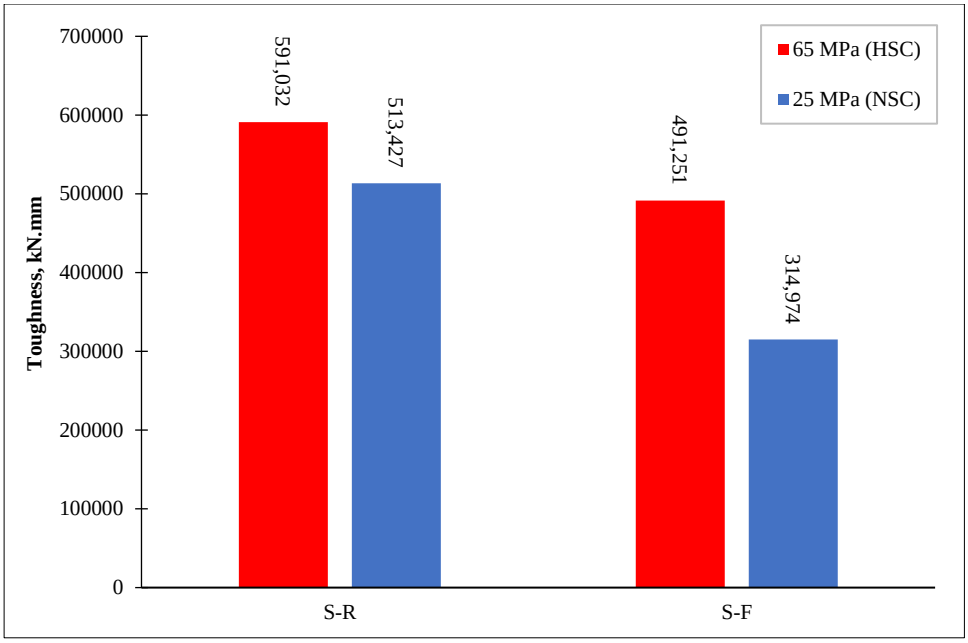

Figure 14. Effect of high temperatures on toughness of the normal and high strength class concrete slab

As a brief summary, all evidentiary evidence has clarified that the high-strength concrete slab can resist fire effects sufficiently compared to the normal concrete. When the concrete strength increased by more than 250%, the resistance to fire effects increased by approximately double in terms of the mentioned indices.

4.2. Behaviour of the Fire-Damaged Slab after Strengthening with CFRP

The load-mid-span deflection behavior of the normal strength-class concrete after strengthening with two different CFRP sheet thicknesses is illustrated in Figure 16. For normal concrete slabs, it can be clearly observed that wrapping with 1.5 mm and 2.5 mm CFRP thicknesses has enhanced maximum load carrying capacity and has been recovered successfully when compared with fire-damaged slabs. While the 1.5 mm CFRP strengthened slab is still incomparable to the reference (undamaged slab). in contrast to the 2.5 mm CFRP thickness layer strengthening, where the load carrying capacity has been successfully recovered. While strengthening the high-strength concrete slab even with a 1.5 mm CFRP layer thickness, it was comparable to the reference slab and, of course, higher than the fire-damaged model, as shown in Figure 17.

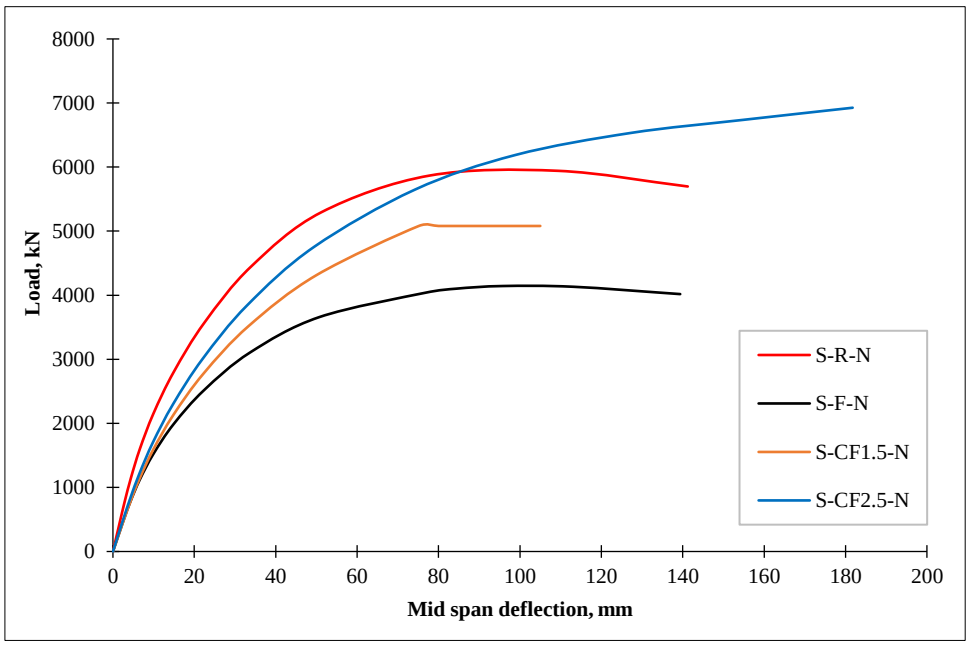

Figure 15. Effect of slab strengthening with two various CFRP jacket thickness on the load- mid span displacement behavior of normal strength concrete

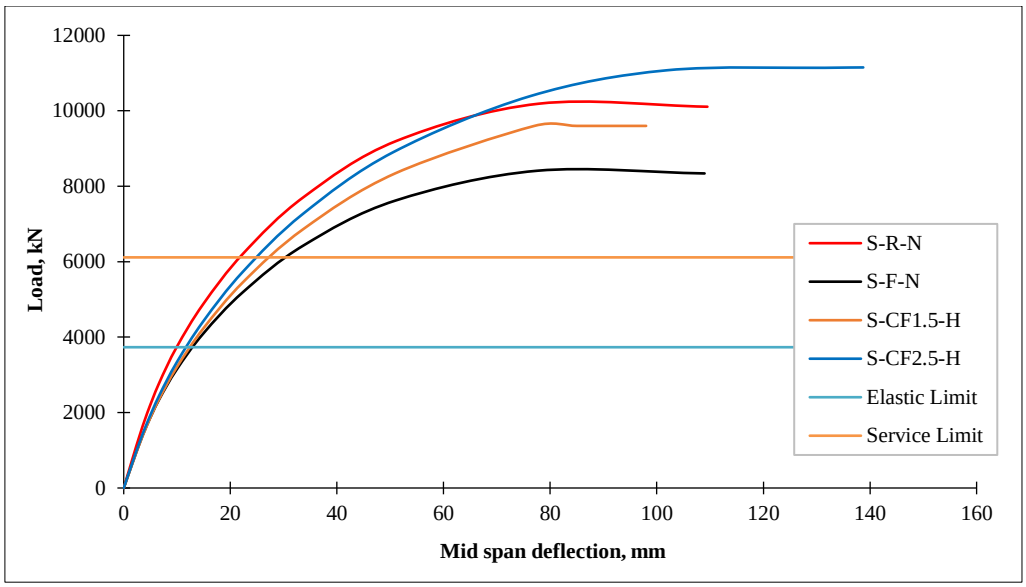

Figure 16. Effect of slab's strengthening with two various CFRP jacket thickness on the load- mid span displacement behavior of high strength concrete

As can be seen in Figure 18, for the high-strength slab, it can be noticed that the load capacity has been recovered at about 85% and fully recovered at 142% for the 1.5 mm and 2.5 mm CFRP thickness layers, respectively. meaning that increasing the CFRP layer 1.6 times, resulted in improving the load carrying capacity by about 1.6 times.

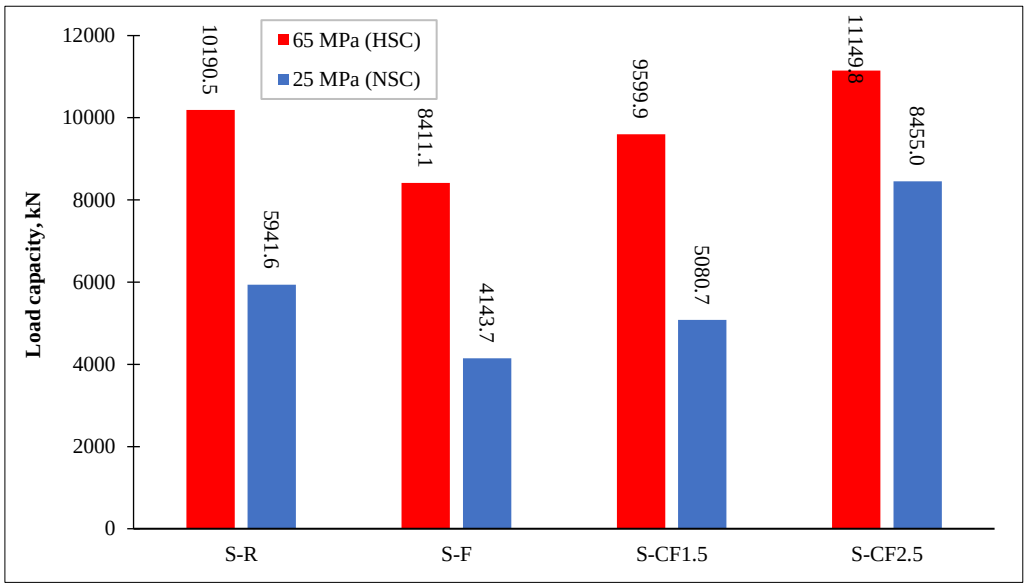

Figure 17. Load carrying capacity comparison between the CFRP strengthened slab and the reference and fire damaged slabs

While for the high-strength slab, approximately both of the CFRP layer thicknesses were successfully recovered to recover the local carrying capacity, more precisely, load capacity has been recovered at about 94% and fully recovered (109%) for 1.5 mm and 2.5 mm CFRP thickness layers, respectively. meaning that increasing the CFRP layer 1.6 times resulted in improving the load carrying capacity by about 1.16 times.

In summary, the effectiveness and contribution of CFRP to enhance the load-carrying capacity of normal-strength slabs were higher than what has been noticed in high-strength slabs by about 140%.

In the case of the stiffness index, neither the normal strength nor the high strength strengthened slabs succeed in recovering the initial stiffness since the stiffness index is largely dependent on the concrete strength property. Overall, for both of the concrete strength classes, the stiffness index of the strengthened slabs was the same as the stiffness value of fire-damaged members. In other words, the stiffness recovery was about 53% and 79% for normal and high-strength concrete slabs, respectively. As a result, it can be concluded that even with increasing the CFRP sheet layer thickness to 166%, the stiffness was the same. Figure 19 shows slab performance in terms of stiffness for the CFRP-wrapped slab members.

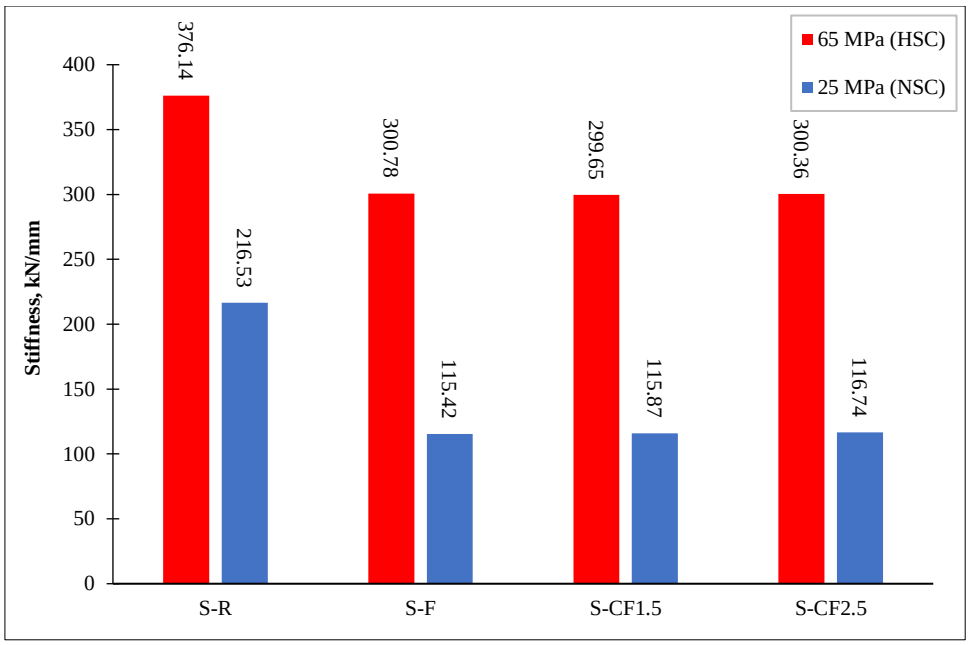

Figure 18. Slab performance in terms of Stiffness for the CFRP wrapped slab members

For the slabs' ductility performance, for a normal concrete slab, the ductility of a 1.5 mm CFRP-strengthened slab was unsuccessfully recovered compared to the reference slab. In other words, the ductility was the same as the fire-damaged slab, and only 80% of the ductility has been recovered. For a 2.5 mm CFRP layer thickness, the ductility was fully recovered (185% higher than the reference slab) and higher than the fire damaged member by about 222%. Which means, in brief, that increasing CFRP layer thickness 1.66 times resulted in enhancing the ductility index 2.25 times.

The CFRP strengthening in high-strength slab members showed lesser efficiency than what I have noticed in normal-strength concrete slabs. 1.5 mm CFRP layer thickness showed comparable value to the fire-damaged member, while full recovery has been achieved for 2.5 mm CFRP layer thickness (133% higher than the reference slab). Which reflects a 144% enhancement in the ductility value for a high-strength slab when increasing the CFRP layer thickness by 166%.

It's worth mentioning that the effectiveness of 1.5 mm CFRP layer thickness was the same on normal and high-strength concrete. In contrast to the 2.5 mm thickness, which showed that the enhancement in the normal strength was higher than the high strength slab by about 1.5 times. Figure 20, shows the performance of a CFRP-strengthened slab in terms of ductility.

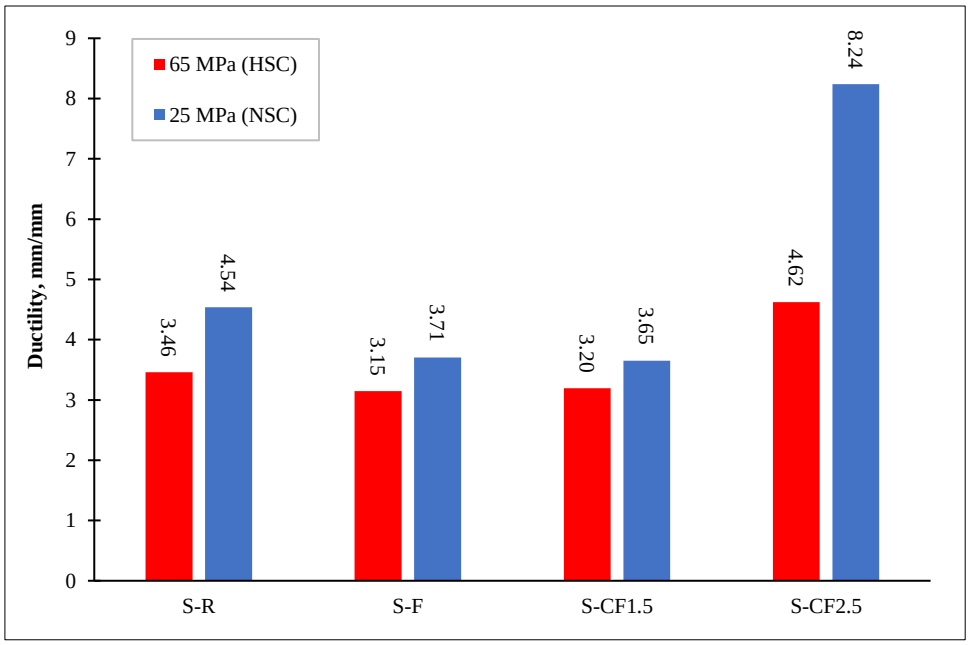

Figure 19. performance of CFRP strengthened slab in terms of ductility

Simulation results of CFRP-treated slabs have shown that 1.5 mm layer thickness was not enough to recover the toughness of the fire-damaged slabs, as can be seen in Figure 21. On the other hand, treating the fire-damaged slabs with a 2.5-mm CFRP layer's thickness succeeded in recovering the toughness of the member sufficiently. For instance, increasing the CFRP layer thickness by 166% resulted in improving the slab's absorption energy by about 581% and 238% for normal and high-strength concrete slabs, respectively. Which means that the contribution of CFRP in a normal strength slab was very effective compared to the high-strength concrete slab and was higher by about more than 200%.

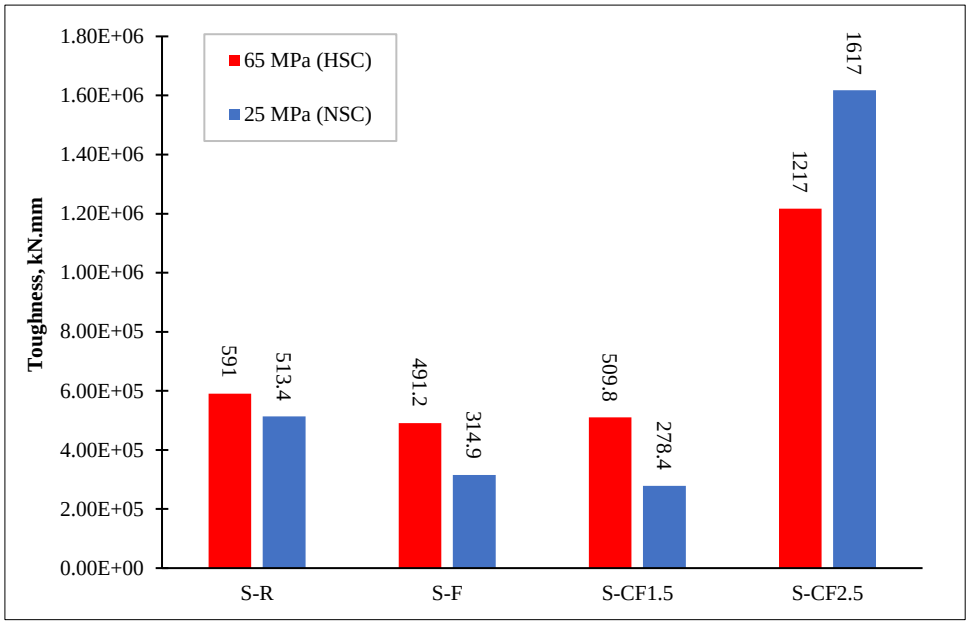

Figure 20. Performance of CFRP strengthened slab in terms of absorption energy

4.3. Behaviour of the Fire-Damaged Slab after Strengthening with SIFCON

The behavior of a SIFCON fire-damaged treated slab (normal strength concrete type) in terms of load displacement behavior is shown in Figure 22. Overall, it can be noticed that treating a normal concrete slab with a 20 mm SIFCON layer thickness resulted in enhancing load displacement curve behavior to be like the reference undamaged slab. In addition, the 30 mm SIFCON-treated slab showed much higher strength than the fire-damaged slab and also higher than the reference slab. Of course, if such an increase happens, other indices, as shall be discussed in detail next, will be sufficiently improved. The same behavior for high-strength slabs of concrete has been observed; see Figure 23.

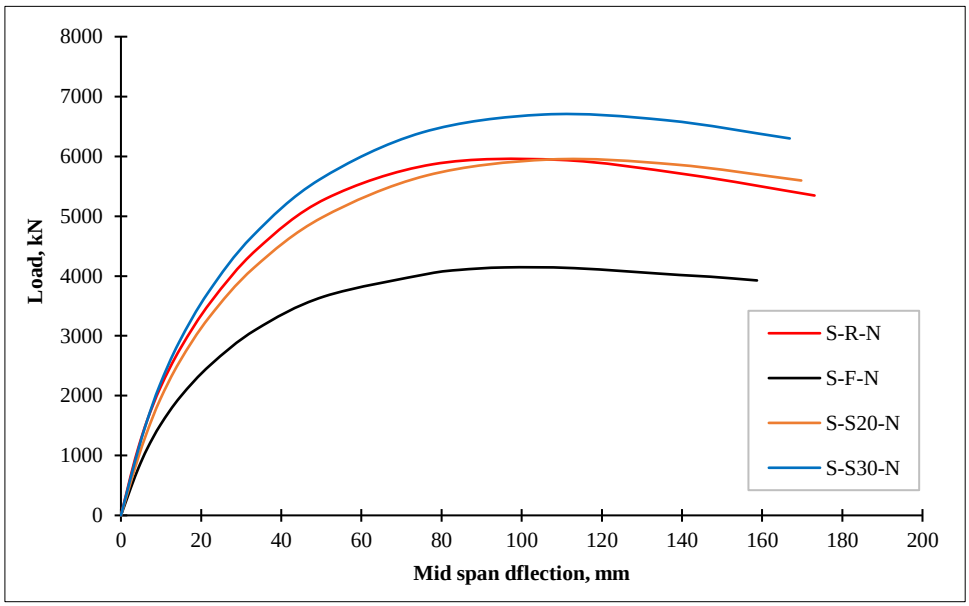

Figure 21. Effect of slab's strengthening with SIFCON jacket on the load- mid span displacement behavior of normal strength concrete slabs

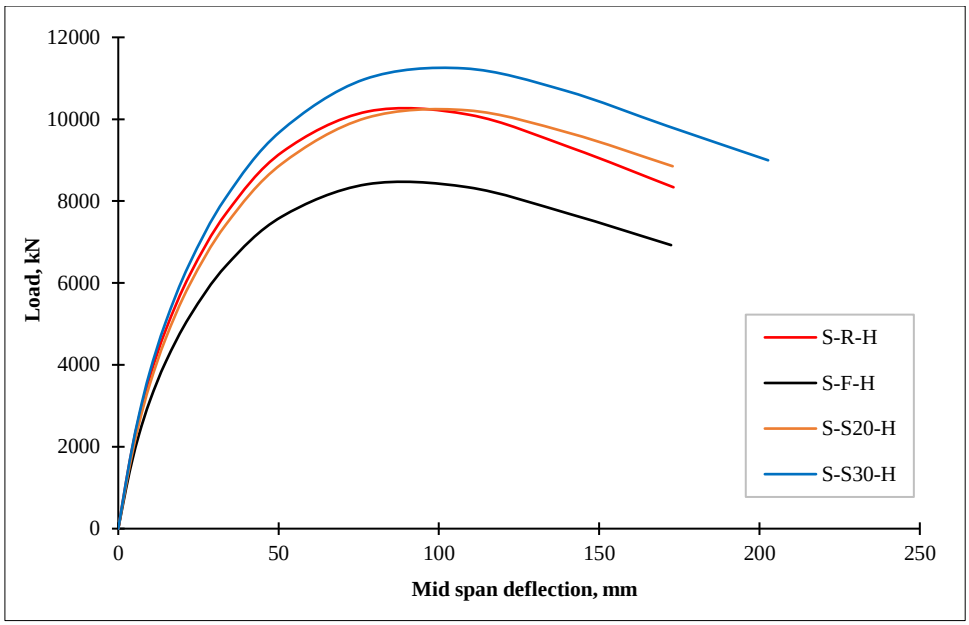

Figure 22. Effect of slab's strengthening with SIFCON jacket on the load- mid span displacement behavior of high strength concrete slabs

The load-mid-span deflection behavior of the normal strength-class concrete after strengthening with two different SIFCON layers' thicknesses is illustrated in Figure 24. For a normal concrete slab, it can be clearly observed that treating with 20 mm and 30 mm CFRP thicknesses enhanced maximum load carrying capacity has been recovered successfully when compared with the reference slab. For normal-strength concrete, increasing the SIFCON layer thickness from 20 mm to 30 mm resulted in improved load carrying capacities of 143% and 161%, respectively, when compared with the fire-damaged slab. Meaning that increasing the SIFCON layer thickness by 150% resulted in improving the load capacity by 112%.

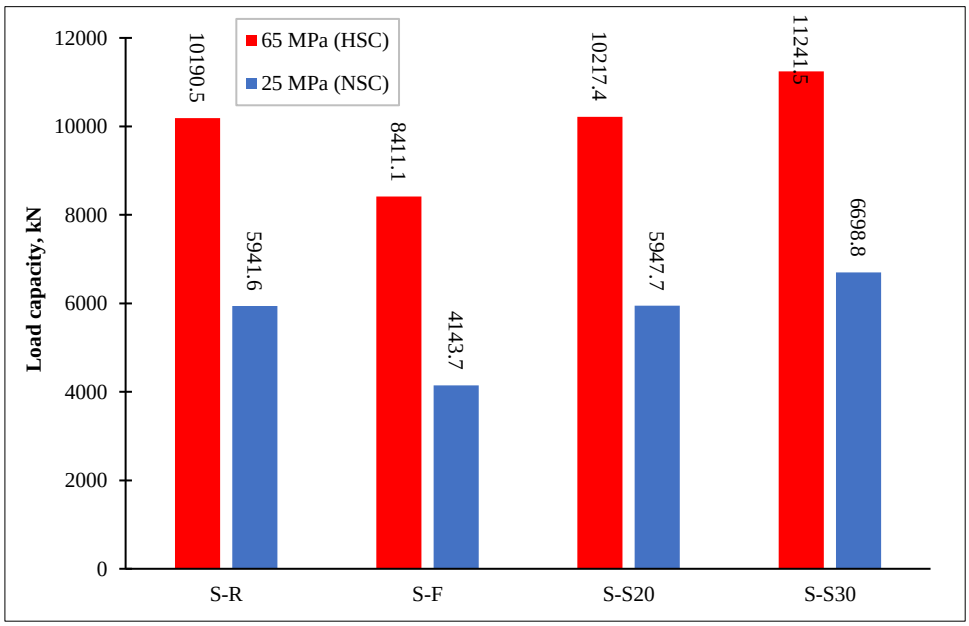

Figure 23. Performance of SIFCON jacket's treated slabs in terms of load capacity index

In the case of high-strength concrete, increasing the SIFCON layer thickness from 20 mm to 30 mm resulted in improving the load carrying capacity by 121% and 131%, respectively, when compared with the fire-damaged slab. Meaning that increasing the SIFCON layer thickness by 150% resulted in improving the load capacity by 108%.

It should be noted that the level of improvement in normal-strength concrete was a little bit higher than what I have noticed in high-strength concrete by about 4%. Overall, it can be said that the concrete strength has a negligible effect on increasing SIFCON layer thickness.

In terms of the stiffness index, it can be observed that the strengthened normal concrete slab with 20 mm SIFCON was unable to reach the reference stiffness value, and the recovery value was about 81%. In contrast to the high-strength concrete slab, where full stiffness recovery has been achieved while treating the fire-damaged slab with a 20-mm SIFCON layer thickness, on the other side, both normal and high-strength concrete slabs treated with a 30 mm SIFCON layer thickness successfully achieved the reference stiffness value.

Overall, it has been noticed that increasing SIFCON layer thickness by about 150% resulted in improving stiffness by about 126% and 125%, respectively, for normal and high-strength concrete slabs. Figure 25, shows the performance of SIFCON jacket-treated slabs in terms of stiffness index. Which means that the concrete strength has no effect on the level of improvement for the stiffness index.

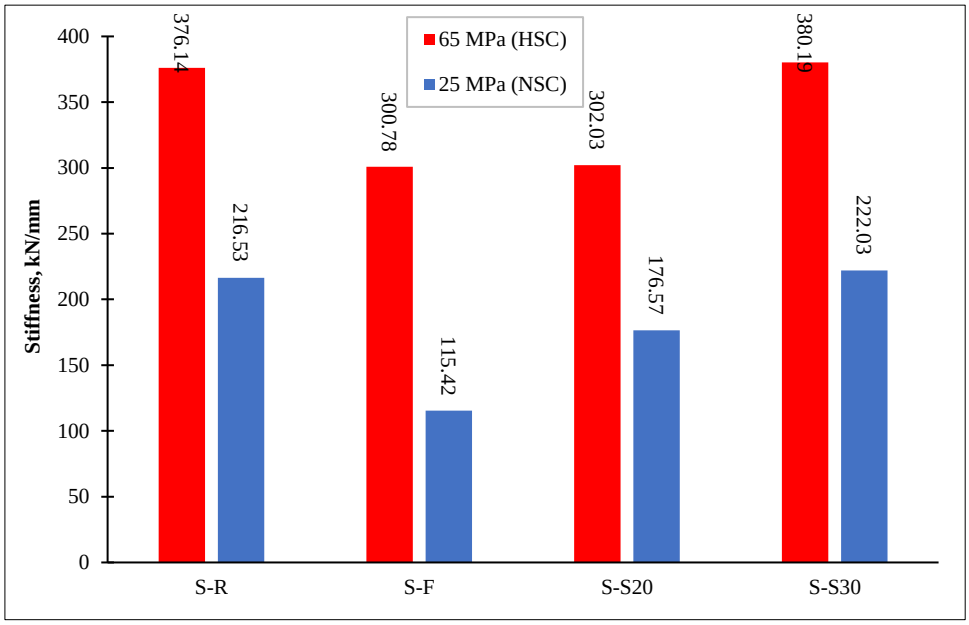

Figure 24. Performance of SIFCON jacket treated slabs in terms of stiffness index

The ductility performance of the SIFCON-treated slabs of concrete is shown in Figure 26. In the figure, it can be observed that both of the SIFCON layer thickness-treated slabs were unable to recover the reference ductility. The recovery percentages were 79.9% and 80.1% for 20 mm and 30 mm SFICON thicknesses, respectively. Which means that increasing the layer thickness of SIFCON has no effect on the performance of a normal-strength slab's ductility. On the other hand, both slabs treated with SIFCON layer thicknesses successfully recovered their stiffness (higher than 142% on average).

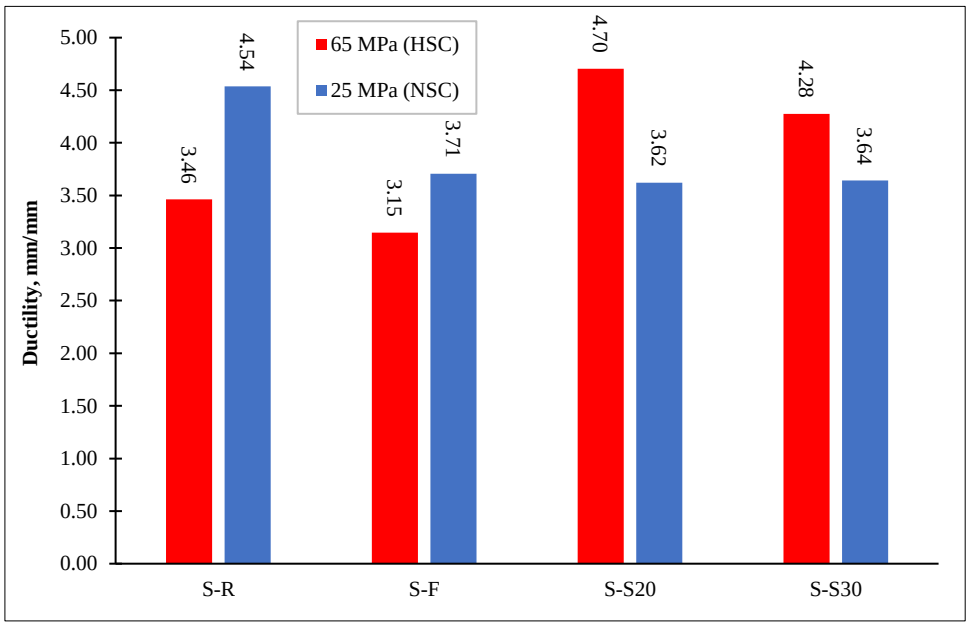

Figure 25. Performance of SIFCON jacket treated slabs in terms of ductility index

Simulation results of SIFCON-treated slabs, as illustrated in Figure 27, have shown significant improvement for the high-strength concrete type in contrast to the normal-strength concrete slabs.

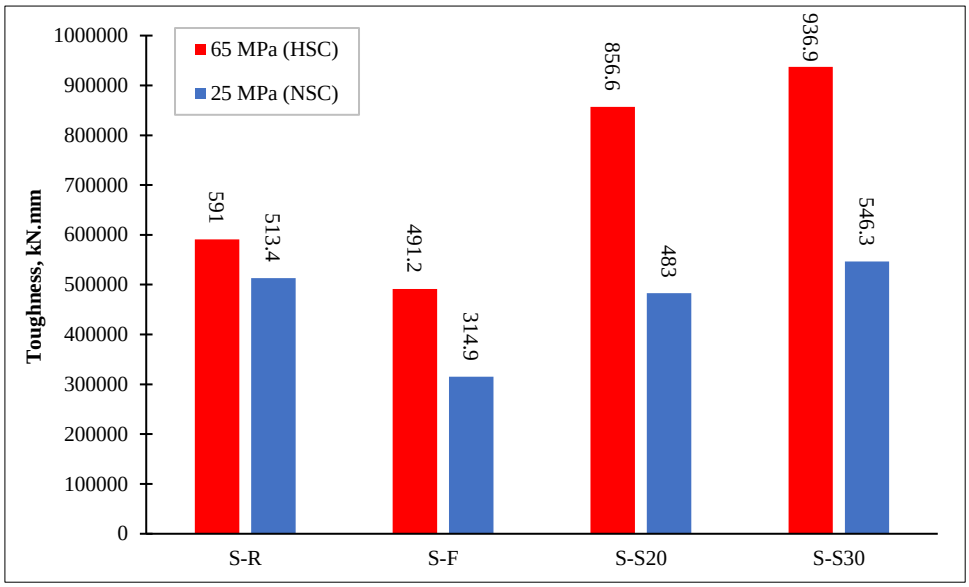

Figure 26. Performance of SIFCON jacket treated slabs in terms of toughness index

For normal concrete slabs, it has been observed that the 20 mm SIFCON treated slab almost achieved the absorption energy index (94%), while the 30 mm SIFCON treated slab reflected full absorption energy recovery (106.5%). While for high-strength concrete slabs, the toughness values were higher than the reference by about 145% and 158%, respectively, for 20 mm and 30 mm SIFCON layer thicknesses. Overall, it can be concluded that increasing SIFCON layer thickness by 150% has no effect on the toughness improvement for normal-strength concrete and a very small increase for the high-strength concrete slab. Moreover, increasing concrete strength 2.6 times reflected a 145% enhancement in the thoroughness index of SIFCON-treated slabs. Table 3 shows the most important results achieved in this study in terms of Stiffness, Ductility and Toughness indicators before and after exposure to high temperatures as well as after strengthening phase.

Table 3. The effect of high temperature on Stiffness, Ductility and Toughness indicators

	Stiffness index		Ductility index		Toughness index	
	NSC	HSC	NSC	HSC	NSC	HSC
R	216.53	376.14	4.54	3.46	513.427	591.032
F	115.42	300.75	3.71	3.15	314.974	491.251
CFRP 1.5 mm	115.87	299.65	3.65	3.20	278.399	509.853
CFRP 2.5 mm	116.74	300.36	8.24	4.62	1617.729	1217.200
SIFCON 20 mm	176.57	302.03	3.52	3.28	483.036	856.665
SIFCON 30 mm	222.03	380.19	2.87	2.94	546.375	936.909

Table 2 reveals the most important results achieved in this study. They are as follows:

- Both normal and high-strength concrete slabs treated with a 30 mm SIFCON layer thickness successfully achieved the reference stiffness value. For both of the concrete strength classes. In the case of the stiffness index in slabs, neither the NSC slabs nor the HSC slabs succeed in recovering the initial stiffness, so it can be concluded that even with increasing the CFRP sheet layer thickness to 166%, the stiffness was the same.
- Both SIFCON layer thickness-treated slabs were unable to recover the reference ductility. The recovery percentages were 79.9% and 80.1% for normal and high strength concrete, respectively. For both normal and high-strength concrete slabs, the 1.5-mm CFRP layer thickness had the same efficiency. Compared to the 2.5 mm thickness, which showed that the improvement in the normal strength was nearly 1.5 times greater than the high-strength slab.
- A 150% increase in SIFCON layer thickness has no impact on toughness improvement for NSC slabs, and it has very little of an impact on HSC slabs. For normal and high-strength concrete slabs, respectively, increasing the CFRP layer thickness by 166% increased the slab's capacity for absorption energy by around 581% and 238%, respectively.

- Treating the fire-damaged NSC slab with 20 mm and 30 mm SIFCON layer thicknesses resulted in enhancing the load capacity by about 143% and 161%, respectively. While treating the fire-damaged HSC slab with 20 mm and 30 mm SIFCON layer thicknesses, they enhance the load capacity by about 121% and 131%, respectively, when compared with the fire-damaged slab. While it can be noticed that the load capacity has been recovered in the NSC slab by about 85% and fully recovered by 142% for the 1.5 mm and 2.5 mm CFRP thickness layers, respectively. In HSC slabs, load capacity has been recovered to about 94% and fully recovered to 109% for 1.5 mm and 2.5 mm CFRP thickness layers.

5. Conclusions

In summary, the key conclusions are that:

- For the normal strength concrete slab, the SIFCON repair with 30 mm thickness improved the strength by 161% compared to the damaged slab. This was the highest improvement of all the repair techniques studied.
- For the high strength concrete slab, the 30 mm thick SIFCON repair improved the strength by 131% compared to the damaged slab, this was the highest improvement achieved.

Due to its composite action with the original concrete, which enables more efficient stress transfer, as well as the presence of discrete fibers that prevent micro cracking and increase toughness, SIFCON can successfully restore and even improve the original strength of fire-damaged concrete slabs. Compared to CFRP, it is less prone to damage at high temperatures. SIFCON's fire resistance, high residual strength, acceptable stiffness, and good bond characteristics allow it to prevent material degradation brought on by fire exposure and restore or even increase the concrete slab's original load-bearing capability.

Theoretical knowledge and numerical data gathered from this study's research can be used to provide design guidelines for SIFCON's best application in post-fire strengthening and restoration of normal- and high-strength concrete structures.

6. Declarations

6.1. Author Contributions

Conceptualization, A.E. and H.A.; methodology, A.E. and H.A.; software, H.A.; validation, A.E. and H.A.; formal analysis, H.A.; investigation, H.A.; resources, H.A.; data curation, H.A.; writing—original draft preparation, H.A.; writing—review and editing, A.E.; supervision, A.E. All authors have read and agreed to the published version of the manuscript.

6.2. Data Availability Statement

The data presented in this study are available in the article.

6.3. Funding

The authors received no financial support for the research, authorship, and/or publication of this article.

6.4. Conflicts of Interest

The authors declare no conflict of interest.

7. References

[1] Zhou, J., & Wang, L. (2019). Repair of Fire-Damaged Reinforced Concrete Members with Axial Load: A Review. Sustainability (Switzerland), 11(4), 963. doi:10.3390/su11040963.

[2] Balamurugan, G., & Viswanathan, T. S. (2020). Evaluation of the effects of orientation and coverage areas of FRP lamination bonded with two-way RC slabs - a modular approach. Civil Engineering and Architecture, 8(4), 706–713. doi:10.13189/cea.2020.080432.

[3] Bezerra, A. C. S., Maciel, P. S., Corrêa, E. C. S., Soares Junior, P. R. R., Aguilar, M. T. P., & Cetlin, P. R. (2019). Effect of High Temperature on the Mechanical Properties of Steel Fiber-Reinforced Concrete. Fibers, 7(12), 100. doi;10.3390/fib7120100.

[4] Zhang, C., Ma, W., Liu, X., Tian, Y., & Orton, S. L. (2019). Effects of high temperature on residual punching strength of slab-column connections after cooling and enhanced post-punching load resistance. Engineering Structures, 199, 109580. doi:10.1016/j.engstruct.2019.109580.

[5] Abdulah, M.D. (2015). Behavior of Reinforced Lightweight Concrete Two Way Slabs Strengthened With CFRP Sheets. Engineering and Technology Journal, 33(8A), 1813–1829. doi:10.30684/etj.2015.108825.

[6] Sui, Z. A., Dong, K., Jiang, J., Yang, S., & Hu, K. (2020). Flexural behavior of fire-damaged prefabricated RC Hollow slabs strengthened with CFRP versus TRM. Materials, 13(11), 2556. doi:10.3390/ma13112556.

[7] Huang, Z., Zhao, Y., Zhang, J., & Wu, Y. (2020). Punching shear behaviour of concrete slabs reinforced with CFRP grids. Structures, 26, 617–625. doi:10.1016/j.istruc.2020.04.047.

[8] Mohan, A., Karthika, S., Ajith, J., dhal, L., & Tholkapiyan, M. (2020). Investigation on ultra-high strength slurry infiltrated multiscale fibre reinforced concrete. Materials Today: Proceedings, 22, 904–911. doi:10.1016/j.matpr.2019.11.102.

[9] Al-Abdalay, N. M., Zeini, H. A., & Kubba, H. Z. (2020). Investigation of the behavior of slurry infiltrated fibrous concrete. Journal of Advanced Research in Fluid Mechanics and Thermal Sciences, 65(1), 109–120.

[10] Carrillo, J., Ramirez, J., & Lizarazo-Marriaga, J. (2019). Modulus of elasticity and Poisson's ratio of fiber-reinforced concrete in Colombia from ultrasonic pulse velocities. Journal of Building Engineering, 23, 18–26. doi:10.1016/j.jobe.2019.01.016.

[11] Panahi, H., & Genikomsou, A. S. (2022). Comparative Investigation of Concrete Plasticity Models for Nonlinear Finite-Element Analysis of Reinforced Concrete Specimens. Practice Periodical on Structural Design and Construction, 27(2), 4021083. doi:10.1061/(asce)sc.1943-5576.0000670.

[12] Raza, A., Khan, Q. U. Z., & Ahmad, A. (2019). Numerical investigation of load-carrying capacity of GFRP-reinforced rectangular concrete members using CDP model in Abaqus. Advances in Civil Engineering, 2019. doi:10.1155/2019/1745341.

[13] Michał, S., & Andrzej, W. (2015). Calibration of the CDP model parameters in Abaqus. The 2015 World Congress on Advances in Structural Engineering and Mechanics (ASEM 15), 25-29, 2015, August, Incheon, Korea.

[14] Le Minh, H., Khatir, S., Abdel Wahab, M., & Cuong-Le, T. (2021). A concrete damage plasticity model for predicting the effects of compressive high-strength concrete under static and dynamic loads. Journal of Building Engineering, 44, 103239. doi:10.1016/j.jobe.2021.103239.

[15] Bakhti, R., Benahmed, B., Laib, A., & Alfach, M. T. (2022). New approach for computing damage parameters evolution in plastic damage model for concrete. Case Studies in Construction Materials, 16, 834. doi:10.1016/j.cscm.2021.e00834.

[16] Nastri, E., & Todisco, P. (2022). Macromechanical Failure Criteria: Elasticity, Plasticity and Numerical Applications for the Non-Linear Masonry Modelling. Buildings, 12(8), 1245. doi:10.3390/buildings12081245.

[17] Anas, S. M., Alam, M., & Shariq, M. (2022). Behavior of two-way RC slab with different reinforcement orientation layouts of tension steel under drop load impact. Materials Today: Proceedings. doi:10.1016/j.matpr.2022.08.509.

[18] Habeeb Albo Sabar, A., & Mansour Kadhum, M. (2022). Numerical modeling of the experimental test for shear strengthened of fire damaged high strength lightweight RC beams with SIFCON jacket. Periodicals of Engineering and Natural Sciences (PEN), 10(2), 512. doi:10.21533/pen.v10i2.2984.

[19] Cai, B., Li, B., & Fu, F. (2020). Finite Element Analysis and Calculation Method of Residual Flexural Capacity of Post-fire RC Beams. International Journal of Concrete Structures and Materials, 14(1), 1-17. doi:10.1186/s40069-020-00428-7.